# Oxygen Atom Transfer, Sulfur Atom Transfer, and Correlated Electron−Nucleophile Transfer Reactions of Oxo- and Thiomolybdenum(IV) Complexes: Synthesis of Oxothiomolybdenum(VI) and (Hydroxo)oxomolybdenum(V) Species

**Charles G. Young,*[1a] Les J. Laughlin,[1a] Silvano Colmanet,[1b] and Sergio D. B. Scrofani[1a]**

School of Chemistry, University of Melbourne, Parkville 3052, Australia, and Australian Radiation Laboratory, Lower Plenty Road, Yallambie 3085, Australia

*Received April 11, 1996*[⊗]

Reaction of $Mo^{IV}O(S_2PR_2)_2$ with K{HB(Pr$^i$pz)$_3$} [HB(Pr$^i$pz)$_3^-$ = hydrotris(isopropylpyrazol-1-yl)borate] in refluxing toluene affords green L*$Mo^{IV}O(S_2PR_2$-*S,S*′) complexes [L* = HB(3-Pr$^i$pz)$_2$(5-Pr$^i$pz)$^-$ = hydrobis(3-isopropylpyrazol-1-yl)(5-isopropylpyrazol-1-yl)borate; R = Pr$^i$, Ph], which are converted upon reaction with boron sulfide in dichloromethane to the yellow thio analogues L*$Mo^{IV}S(S_2PR_2$-*S,S*′). Crystals of L*$Mo^{IV}O(S_2PPr^i_2)$ are monoclinic, space group $P2_1/n$, with $a$ = 10.024(2) Å, $b$ = 20.999(9) Å, $c$ = 15.368(5) Å, $\beta$ = 100.57(2)°, $V$ = 3180(2) Å$^3$, and $Z$ = 4. Crystals of L*$Mo^{IV}S(S_2PPh_2)$ are monoclinic, space group $P2_1$, with $a$ = 10.801(8) Å, $b$ = 13.100(5) Å, $c$ = 12.023(9) Å, $\beta$ = 99.56(10)°, $V$ = 1678(2) Å$^3$, and $Z$ = 2. The mononuclear, distorted-octahedral complexes are isostructural and are composed of a terminal chalcogenide ligand [Mo═O = 1.671(3) Å, Mo═S = 2.126(3) Å], a bidentate dithiophosphinate-*S,S*′ ligand, and a facial, tridentate L* ligand. In both cases the 5-isopropylpyrazole group is bound *trans* to the Mo═E group (E = O, S). Oxygen atom transfer to L*$Mo^{IV}S(S_2PR_2)$ and sulfur atom transfer to L*$Mo^{IV}O(S_2PR_2)$ produce the oxo−thio−Mo(VI) complexes L*$Mo^{VI}OS(S_2PR_2$-*S*). NOESY experiments confirm that the 5-isopropylpyrazole group is *trans* to the Mo═O group in these chiral complexes. Ferrocenium oxidation of L*$Mo^{IV}E(S_2PR_2)$ yields the corresponding oxo− and thio−Mo(V) complexes [L*$Mo^{V}E(S_2PR_2$-*S,S*′)]$^+$, respectively; the [L*$Mo^{V}O(S_2PR_2$-*S,S*′)]$^+$ complexes react with water to produce (hydroxo)oxo−Mo(V) species, L*$Mo^{V}O(OH)(S_2PR_2$-*S*), while the thio analogues are decomposed by water. The complex L′$Mo^{V}OCl_2$ [L′ = HB(3-Pr$^i$pz)$_3^-$ = hydrotris(3-isopropylpyrazol-1-yl)borate] was prepared by reacting L′$Mo^{VI}O_2Cl$ with $PPh_3$ in dichloromethane; this complex does not react with sulfiding agents to produce the analogous thio complex.

## Introduction

The simple replacement of a terminal oxo ligand by a terminal thio[2] ligand is a reaction plagued by practical limitations; the facile reduction of high-valent metal centers by sulfide and the formation of polynuclear $\mu$-thio complexes usually conspire to prevent clean reactions. Nevertheless, this reaction has played a vital role in the generation of $[Mo^{VI}OS]^{2+}$, $[Mo^{V}OS]^{+}$ and $[Mo^{V}O(SH)]^{2+}$ complexes, some of which are important models for the molybdenum centers formed during turnover of xanthine oxidase and xanthine dehydrogenase.[3−5] Most oxo−thio−Mo(VI) complexes have been produced by sulfidation of oxo complexes; examples include the oxothiomolybdates, $[Mo^{VI}O_{4-n}S_n]^{2-}$,[6] the Wieghardt complexes $Mo^{VI}OS(ONR_2)_2$,[7] and the organometallic species ($\eta^5$-$C_5Me_5$)$Mo^{VI}OS(CH_2SiMe_3)$.[8] Generally, however, sulfidation of oxo−Mo(VI) complexes does not lead to clean replacement of an oxo ligand by a thio ligand; for example, sulfidation of $LMo^{VI}O_2X$ [L = HB(Me$_2$pz)$_3^-$;[9] X = F, Cl, Br, NCS] and $[Mo^{VI}O(S_2CNR_2)_3]^+$ leads to reduction and formation of $LMo^{IV}(S_4)X$[10] and $[Mo^{V}_2(\mu\text{-}S_2)_2(S_2CNR_2)_4]^{2+}$,[11] respectively. At the Mo(V) level, models for the Very Rapid and Rapid centers of xanthine oxidase[12] were generated *in situ* upon reaction of *cis*-dioxo−Mo(V) complexes with $SH^-$,[13−17] and the conversion of $LMo^{V}OCl_2$ to $LMo^{V}SCl_2$ was achieved using boron sulfide.[18]

⊗ Abstract published in *Advance ACS Abstracts,* August 1, 1996.

(1) (a) University of Melbourne. (b) Australian Radiation Laboratory.
(2) Thio is the recommended and preferred name for the formally $S^{2-}$ ligand. In CAS index nomenclature this name is modified to thioxo when a terminal ligand is specified, while $\mu_x$-thio specifies bridging $S^{2-}$ ligands. In this paper we use the term thio to refer to the terminal monatomic ligand in Mo═S units. See: Block, B. P.; Powell, W. H.; Fernelius, W. C. *Inorganic Chemical Nomenclature*; American Chemical Society: Washington, 1990; p 41. *Chemical Abstracts Index Guide*; Chemical Abstracts Service: Columbus, OH, 1994; Appendix 4.
(3) Enemark, J. H.; Young, C. G., *Adv. Inorg. Chem.* **1993**, *40*, 1 and references therein.
(4) Young, C. G.; Wedd, A. G. *Encyclopedia of Inorganic Chemistry*; King, R. B. Ed.; Wiley, Chichester, U.K., 1994; p 2330 and references therein.
(5) Pilato, R. S.; Stiefel, E. I. In *Inorganic Catalysis*; Reedijk, J., Ed.; Marcel Dekker: New York, 1993; p 131 and references therein.
(6) Diemann, E.; Müller, A. *Coord. Chem. Rev.* **1973**, *10*, 79.
(7) (a) Hofer, E.; Holzbach, W.; Wieghardt, K. *Angew. Chem., Int. Ed. Engl.* **1981**, *20*, 282. (b) Wieghardt, K.; Hahn, M.; Weiss, J.; Swiridoff, W. *Z. Anorg. Allg. Chem.* **1982**, *492*, 164. (c) Bristow, S.; Collison, D.; Garner, C. D.; Clegg, W. *J. Chem. Soc., Dalton Trans.* **1983**, 2495. (d) Traill, P. R.; Tiekink, E. R. T.; O'Connor, M. J.; Snow, M. R.; Wedd, A. G. *Aust. J. Chem.* **1986**, *39*, 1287.
(8) Faller, J. W.; Ma, Y. *Organometallics* **1989**, *8*, 609.
(9) Abbreviations: L = HB(Me$_2$pz)$_3^-$ = hydrotris(3,5-dimethylpyrazol-1-yl)borate; L* = HB(3-Pr$^i$pz)$_2$(5-Pr$^i$pz)$^-$ = hydrobis(3-*i*-propylpyrazol-1-yl)(5-*i*-propylpyrazol-1-yl)borate; L′ = HB(3-Pr$^i$pz)$_3^-$ = hydrotris(3-*i*-propylpyrazol-1-yl)borate; Cp = $\eta^5$-cyclopentadienyl; OAT = oxygen atom transfer; SAT = sulfur atom transfer; CENT = correlated electron−nucleophile transfer; CEPT = coupled electron−proton transfer; CEET = coupled electron−electrophile transfer; NOESY = nuclear Overhauser spectroscopy; TOCSY = total correlation spectroscopy.
(10) Young, C. G.; McInerney, I. P.; Bruck, M. A.; Enemark, J. H. *Inorg. Chem.* **1990**, *29*, 412.
(11) (a) Kocaba, T. O.; Young, C. G.; Tiekink, E. R. T. *Inorg. Chim. Acta* **1990**, *174*, 143. (b) Young, C. G.; Kocaba, T. O.; Yan, X. F. Tiekink, E. R. T.; Wei, L.; Murray, H. H., III; Coyle, C. L.; Stiefel, E. I. *Inorg. Chem.* **1994**, *33*, 6252.
(12) Bray, R. C. *Q. Rev. Biophys.* **1988**, *21*, 299.
(13) Hinshaw, C. J.; Spence, J. T. *Inorg. Chim. Acta* **1986**, *125*, L17.
(14) Dowerah, D.; Spence, J. T.; Singh, R.; Wedd, A. G.; Wilson, G. L.; Farchione, F.; Enemark, J. H.; Kristofzski, J.; Bruck, M. *J. Am. Chem. Soc.* **1987**, *109*, 5655.
(15) Wilson, G. L.; Greenwood, R. J.; Pilbrow, J. R.; Spence, J. T.; Wedd, A. G. *J. Am. Chem. Soc.* **1991**, *113*, 6803.

S0020-1669(96)00403-X CCC: $12.00 

For Mo(IV) the utility of the oxo/thio exchange reaction is exemplified by the conversion using boron sulfide of $LMo^{IV}O(S_2CNR_2)$ into $LMo^{IV}S(S_2CNR_2)$.[19]

Many examples of oxygen atom transfer (OAT) to oxo−Mo(IV) complexes have been documented;[20] the conversion of oxo−Mo(IV) trispyrazolylborate complexes to *cis*-dioxo−Mo(VI) complexes (eq 1, R = alkyl, aryl, alkoxy) is most pertinent to the work described herein.[17,21,22] Recently, we reported a related strategy, viz., sulfur atom transfer (SAT) to oxo−Mo(IV) complexes (eq 2), for the synthesis of oxo−thio−Mo(VI)

$$LMo^{IV}O(S_2PR_2\text{-}S,S') + [O] \rightarrow LMo^{VI}O_2(S_2PR_2\text{-}S) \quad (1)$$

$$LMo^{IV}O(S_2PR_2\text{-}S,S') + [S] \rightarrow LMo^{VI}OS(S_2PR_2\text{-}S) \quad (2)$$

$$LMo^{IV}S(S_2PR_2\text{-}S,S') + [O] \rightarrow LMo^{VI}OS(S_2PR_2\text{-}S) \quad (3)$$

complexes.[23] A complementary approach to oxo−thio−Mo(VI) complexes involves OAT to suitable thio−Mo(IV) complexes (eq 3). The ambidentate nature of the dithioacid ligands facilitates the reactions in eqs 1−3 and, where oxo−thio−Mo(VI) species are generated, permits the stabilization of the $[MoOS]^{2+}$ center via a weak S··S interaction.[23] To our knowledge, there are no reports of reactions of the type represented by eq 3, and our attempts to prepare the necessary $LMo^{IV}S(S_2PR_2)$ precursors have to date failed.[21] Here, we report the synthesis of the oxo−Mo(IV) complexes $L^*Mo^{IV}O(S_2PR_2\text{-}S,S')$ [L* = $HB(3\text{-}Pr^ipz)_2(5\text{-}Pr^ipz)^-$;[9] R = $Pr^i$, Ph], their conversion to the corresponding thio complexes, $L^*Mo^{IV}S(S_2PR_2\text{-}S,S')$, and the synthesis or generation therefrom of oxo−thio−Mo(VI) and (hydroxo)oxo−Mo(V) species of biological relevance.[3−5] We also describe the synthesis and properties of $L'MoOCl_2$, where L′ = $HB(3\text{-}Pr^ipz)_3^-$.[9] The significance of the work lies in (i) the use of structural and spectroscopic methods, particularly NOESY and TOCSY,[9] to define the regio- and stereoisomeric forms of $K\{HB(Pr^ipz)_3\}$ and various molybdenum complexes, (ii) the achievement of the clean replacement of an oxo ligand by a thio ligand in complexes containing an ambidentate S-donor co-ligand, which permitted (iii) the first demonstration of OAT to thio−Mo(IV) complexes to form stable, isolable oxo−thio−Mo(VI) complexes, and (iv) the generation *in situ* of oxo− and thio−Mo(V) complexes, including (hydroxo)oxo−Mo(V) species formed by correlated electron−nucleophile transfer or CENT[17,21] reactions (Scheme 1).

**Scheme 1**

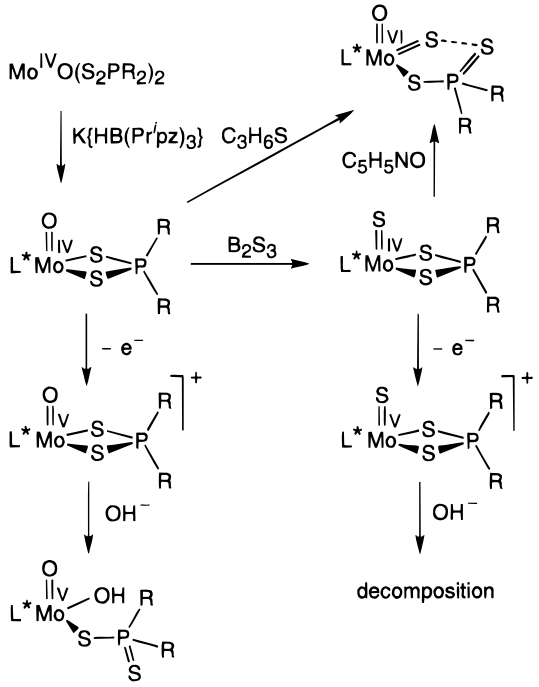


## Experimental Section

**Materials and Methods.** All reactions were performed under a dinitrogen atmosphere using standard Schlenk techniques. Solvents were dried, deoxygenated, and doubly-distilled according to Perrin *et al.*[24] All other chemicals were AR grade or better and were used without further purification; boron sulfide was obtained from Morton Thiokol. The starting materials, $K\{HB(Pr^ipz)_3\}$,[25,26] L′$MoO_2Cl$,[16] $HS_2PR_2$ (R = $Pr^i$, Ph),[27] $MoO_2(S_2PR_2)_2$ and $MoO(S_2PR_2)_2$,[28] and $[FeCp_2]PF_6$[29] were prepared by literature methods. Mass spectra were recorded on a Vacuum Generators VG ZAB 2HF mass spectrometer. Infrared spectra were measured on a Perkin−Elmer FT 1430 spectrophotometer. Electronic spectra were obtained on Shimadzu UV-240 and Hitachi 150−20 UV spectrophotometers. EPR spectra were run on Bruker FT ECS-106 and Varian E-line spectrometers using 1,1-diphenyl-2-picrylhyrazyl as standard. Electrochemical experiments were performed on a Cypress Electrochemical System II with a 3 mm glassy carbon working electrode and platinum working and reference electrodes. Solutions of the complexes (1−2 mM) in 0.1 M $NBu^n_4BF_4$/acetonitrile were employed, and potentials were referenced to internal ferrocene. Potentials are reported relative to the saturated calomel electrode (SCE). Chromatography was performed on a 50 cm column (2 cm dia.) of Merck Art. 7734 Kieselgel 60. Microanalyses were performed by Atlantic Microlabs, Norcross, GA.

$^1H$-, $^1H\{^{31}P\}$- and $^{31}P\{^1H\}$-NMR spectra were recorded on Varian FT Unity 300 (1-D) and Unity-Plus 400 MHz (2-D) spectrometers; all spectra were recorded between 293 and 303 K in $CDCl_3$. Proton and $^{31}P$ chemical shifts were referenced to internal $CHCl_3$ and external 85% $H_3PO_4$, respectively. All 2-D NMR experiments were acquired in the phase-sensitive mode with quadrature detection in the F1 dimension achieved by the States method.[30] In general, 2048 complex points were acquired in F2 with 200−400 increments and 16−32 scans per slice

(16) Xiao, Z.; Bruck, M. A.; Doyle, C.; Enemark, J. H.; Grittini, C.; Gable, R. W.; Wedd, A. G.; Young, C. G. *Inorg. Chem.* **1995**, *34*, 5950.
(17) Laughlin, L. J.; Young, C. G. *Inorg. Chem.* **1996**, *35*, 1050.
(18) Young, C. G.; Enemark, J. H.; Collison, D.; Mabbs, F. E. *Inorg. Chem.* **1987**, *26*, 2925.
(19) Young, C. G.; Roberts, S. A.; Ortega, R. B.; Enemark, J. H. *J. Am. Chem. Soc.* **1987**, *109*, 2938.
(20) (a) Holm, R. H. *Chem. Rev.* **1987**, *87*, 1401. (b) Holm, R. H. *Coord. Chem. Rev.* **1990**, *100*, 183.
(21) Laughlin, L. J. Ph.D. Dissertation, University of Melbourne, 1993.
(22) Roberts, S. A.; Young, C. G.; Cleland, W. E., Jr.; Ortega, R. B.; Enemark, J. H. *Inorg. Chem.* **1988**, *27*, 3044.
(23) Eagle, A. A.; Laughlin, L. J.; Young, C. G.; Tiekink, E. R. T. *J. Am. Chem. Soc.* **1992**, *114*, 9195.
(24) Perrin, D. D.; Armarego, W. L. F. *Purification of Laboratory Chemicals*, 3rd ed.; Pergamon: Oxford, England, 1988.
(25) Trofimenko, S.; Calabrese, J. C.; Domaille, P. J.; Thompson, J. S. *Inorg. Chem.* **1989**, *28*, 1091.
(26) We have preliminary infrared and $^1H$ NMR evidence that in solution and the solid state (over periods of days and weeks, respectively) $K\{HB(Pr^ipz)_3\}$, originally isolated as KL′,[25] undergoes a 1,2-boratropic shift to form KL*. In our experience, the nature (fresh or aged) of the ligand employed in reactions does not influence the products and their yields. Rather, facile ligand rearrangements ensure the formation of the least sterically encumbered product compatible with a particular coordination sphere, viz., the products appear to be under thermodynamic control.
(27) (a) Christen, P. J.; van der Linde, L M.; Hooge, F. N. *Recl. Trav. Chim. Pays-Bas* **1959**, *78*, 161. (b) Corbin, J. L.; Newton, W. E. *Org. Prep. Proc. Int.* **1975**, *7*, 309.
(28) Chen, G. J.-J.; McDonald, J. W.; Newton, W. E. *Inorg. Chem.* **1976**, *15*, 2612.
(29) Desbois, M.-H.; Astruc, D. *New J. Chem.* **1989**, *13*, 595.
(30) States, D. J.; Haberkorn, R. A.; Ruben, D. J. *J. Magn. Reson.* **1982**, *48*, 286.

in F1. NOESY[31] spectra were acquired using a range of mixing times (250−600 ms). TOCSY[32] spectra were acquired with a mixing time of 40 ms using the MLEV-17 mixing scheme flanked by 200 $\mu$s trim pulses. Both NOESY and TOCSY spectra were acquired with and without $^{31}$P decoupling during F2. Spectra were generally processed using 60−90° shifted square sine bell windows in both dimensions and zero filling to 1024 points in F1.

**Preparation of Complexes. L*Mo$^{IV}$O(S$_2$PPr$^i_2$-*S,S′*).** A toluene solution (40 mL) of $MoO_2(S_2PPr^i_2)_2$ (1.91 g, 3.89 mmol) and $PPh_3$ (1.12 g, 4.28 mmol) was refluxed for 1 h. Upon cooling, the mixture was treated with K{HB(Pr$^i$pz)$_3$} (1.48 g, 3.9 mmol) and then refluxed for a further 12 h. The mixture was hot-filtered, the filtrate evaporated to dryness, and the residue column chromatographed using dichloromethane as eluent. The predominant green fraction ($R_f \sim 0.7-0.8$) was collected and recrystallized from dichloromethane/methanol as green crystals. Yield: 1.41 g (58%).

Anal. Calcd for $C_{24}H_{42}BMoN_6OPS_2$: C, 45.58; H, 6.69; N, 13.29; S, 10.14. Found: C, 45.68; H, 6.68; N, 13.28; S, 10.10. IR (KBr): 2950 s, 2900 m, 2850 m, $\nu$(BH) 2500 m, 1510 s, 1480 m, 1460 m, 1400 s, 1380 s, 1360 m, 1310 m, 1240 w, 1190 s, 1130 w, 1100 w, 1090 w, 1060 m, 1040 m, 1010 m, $\nu$(MoO) 955 s, 880 w, 800 m, 770 s, 730 s, 670 s, 600 w, 515 w cm$^{-1}$.

**L*Mo$^{IV}$O(S$_2$PPh$_2$-*S,S′*).** A toluene solution (40 mL) of $MoO_2(S_2PPh_2)_2$ (0.815 g, 1.3 mmol) and $PPh_3$ (0.341 g, 1.3 mmol) was refluxed for 45 min. The mixture was allowed to cool to room temperature and then treated with K{HB(Pr$^i$pz)$_3$} (0.54 g, 1.43 mmol) and refluxed for a further 60 min. The reaction was then filtered and the filtrate evaporated to dryness. The residue was dissolved in dichloromethane and column chromatographed using dichloromethane as eluent. The main green fraction ($R_f \sim 0.7-0.8$) was collected and the complex recrystallized from dichloromethane/methanol to afford the light-green crystalline product. Yield: 0.58 g (65%).

Anal. Calcd for $C_{30}H_{38}BMoN_6OPS_2$: C, 51.44; H, 5.47; N, 12.00; S, 9.15. Found: C, 51.35; H, 5.52; N, 11.92; S, 9.20. IR (KBr): 2970 s, 2920 m, 2870 m, $\nu$(BH) 2500 m, 1510 s, 1490 m, 1460 w, 1440 m, 1400 m, 1380 s, 1360 m, 1310 m, 1240 w, 1190 s, 1100 m, 1070 m, 1050 m, 1020 m, $\nu$(MoO) 955 s, 800 w, 780 s, 750 s, 740 s, 710 s, 690 m, 640 m, 615 m, 570 s, 480 w cm$^{-1}$.

**L*Mo$^{IV}$S(S$_2$PPr$^i_2$-*S,S′*).** A solution of L*MoO(S$_2$PPr$^i_2$) (1.0 g, 1.58 mmol) in dichloromethane (25 mL) was treated with boron sulfide (1.0 g, 8.5 mmol) and the mixture stirred at ambient temperature for at least 4 h (progress of the reaction was monitored by TLC). The reaction was filtered in air through a silica plug which was washed copiously with dichloromethane. The combined filtrate and washings were evaporated to dryness and the residue recrystallized from dichloromethane/methanol to afford yellow-brown crystals. Yield: 0.53 g (50%).

Anal. Calcd for $C_{24}H_{42}BMoN_6PS_3$: C, 43.17; H, 6.35; N, 12.16; S, 14.21. Found: C, 42.98; H, 6.34; N, 12.36; S, 14.10. IR (KBr): 2950 s, 2920 m, 2850 m, $\nu$(BH) 2480 m, 1510 s, 1480 m, 1460 m, 1400 s, 1380 s, 1360 m, 1310 m, 1240 w, 1190 s, 1140 w, 1110 w, 1090 w, 1060 m, 1040 m, 1020 m, 950 w, 880 w, 800 m, 770 s, 730 s, 670 s, 640 m, 620 m, $\nu$(MoS) 515 m cm$^{-1}$.

**L*Mo$^{IV}$S(S$_2$PPh$_2$-*S,S′*).** A mixture of L*MoO(S$_2$PPh$_2$) (0.15 g, 0.214 mmol) and boron sulfide (0.126 g, 1.07 mmol) in dichloromethane (20 mL) was stirred at ambient temperature for 6 h, whereupon the mixture was filtered aerobically, evaporated to dryness, and twice-recrystallized from dichloromethane/methanol to afford yellow-gold crystals. Yield: 0.07 g (47%).

Anal. Calcd for $C_{30}H_{38}BMoN_6PS_3$: C, 50.28; H, 5.35; N, 11.73; S, 13.42. Found: C, 50.21; H, 5.42; N, 11.65; S, 13.49. IR (KBr): 2950 s, 2920 m, 2850 m, $\nu$(BH) 2500 m, 1510 s, 1490 m, 1460 m, 1430 m, 1400 s, 1380 s, 1360 m, 1310 m, 1290 w, 1260 w, 1190 s, 1100 m, 1060 m, 1040 m, 1020 m, 950 w, 800 w, 780 s, 730 s, 710 s, 690 m, 670 s, 640 m, 610 m, 570 s, $\nu$(MoS) 515 w cm$^{-1}$.

**L*MoOS(S$_2$PPr$^i_2$-*S*). Method 1. SAT to L*MoO(S$_2$PPr$^i_2$).** A mixture of L*MoO(S$_2$PPr$^i_2$) (0.12 g, 0.19 mmol) and propylene sulfide (0.4 mL, 5 mmol) in dichloroethane (10 mL) was stirred for 1 week at 55 °C. The reaction mixture was then evaporated to dryness, redissolved in toluene, and column chromatographed (silica/toluene) to give an orange fraction, which was recrystallized from dichloromethane/methanol. Yield: 0.10 g (80%).

**Method 2. OAT to L*MoS(S$_2$PPr$^i_2$).** A mixture of L*MoS(S$_2$PPr$^i_2$) (0.1 g, 0.154 mmol) and pyridine *N*-oxide (0.03 g, 0.315 mmol) in toluene (10 mL) was stirred for 3 days at 55 °C. The reaction mixture was evaporated to dryness and the residue column chromatographed (silica/toluene) to yield an orange fraction which was recrystallized from dichloromethane/methanol. Yield: 0.10 g (90%).

**L*MoOS(S$_2$PPh$_2$-*S*).** Methods 1 and 2 above were adapted to the synthesis of this compound. Yields were ca. 70% and 80%, respectively.

**L*Mo(S$_4$)(S$_2$PPr$^i_2$-*S*).** Reaction of L*MoS(S$_2$PPr$^i_2$) with dry (4 Å sieved) dioxygen gas in toluene at 50 °C for 4 days produced seven species; those identified were L*MoOS(S$_2$PPr$^i_2$) (40%), L*MoO(S$_2$PPr$^i_2$) (30%), and blue L*Mo(S$_4$)(S$_2$PPr$^i_2$) (5%). The latter was isolated by subjecting the evaporated reaction mixture to column chromatography (silica/$CH_2Cl_2$). NMR ($CDCl_3$) (according to group): C*H*Me$_2$ of L*, $\delta$ −0.96, 3.50, and 3.95 (each sep, 1H, $^3J$ = 7 Hz); CH*Me*$_2$ of L*, $\delta$ 0.22, 0.27, 1.28, 1.34, 1.36, and 1.75 (each d, 3H, $^3J$ = 7 Hz); 4-C*H*, $\delta$ 5.30, 6.35, and 6.50 (each d, 1H, $^3J$ = 2 Hz); 3- and 5-C*H*, $\delta$ 7.20, 7.95, and 9.70 (each d, 1H, $^3J$ = 2 Hz); PCH*Me*$_2$, $\delta$ −0.13, 0.27, 0.32, and 0.57 (dd, 3H, $^3J$ = 7 Hz, $J_{PH}$ = 17 Hz); PC*H*Me$_2$, $\delta$ 1.00 and 1.20 (obscured) (each ds, 1H, $^3J$ = 7 Hz, $J_{PH}$ = 7 Hz). $^{31}$P{$^1$H} NMR ($CDCl_3$): $\delta$ 116.

**L′Mo$^{V}$OCl$_2$.** A mixture of L′$MoO_2Cl$ (0.5 g, 1.0 mmol) and $PPh_3$ (0.288 g, 1.1 mmol) in dichloromethane (25 mL) was stirred at ambient temperature for 1 day. After this period, the reaction volume was reduced to ca. 5 mL and then the mixture was treated with $CH_3CN$ (30 mL) to afford light green crystals, which were filtered and washed with $CH_3CN$. Yield: 0.28 g (54%). IR (KBr): 2970 m, $\nu$(BH) 2500 m, 1505 s, 1460 w, 1440 w, 1400 s, 1380 s, 1360 s, 1290 s, 1240 w, 1200 s, 1170 s, 1150 s, $\nu$(MoO) 975 s, 800 m, 780 m, 730 s, 650 w, 630 w, $\nu$($MoCl_2$) 320 and 310 w cm$^{-1}$.

**Crystallographic Studies.** Crystals of L*MoO(S$_2$PPr$^i_2$) and L*MoS(S$_2$PPh$_2$) were grown by slow diffusion of methanol into saturated dichloromethane solutions of the compounds. Unit-cell parameters were obtained at 296 K by least-squares refinement of 2$\theta$ values measured with Cu K$\alpha$ radiation for 30 independent reflections. Integrated intensities were measured on a Siemens AED diffractometer with nickel-filtered Cu K$\alpha$ radiation. Data were measured to a maximum (sin $\theta$)/k$\alpha$ = 0.613 Å$^{-1}$. Three reflections, monitored every 50 reflections, showed no significant variation in intensities. The intensities were corrected for Lorentz and polarization effects and for absorption.[33] Crystallographic data are summarized in Table 1.

**Table 1.** Crystallographic Data for L*MoO(S$_2$PPr$^i_2$) and L*MoS(S$_2$PPh$_2$)

| | L*MoO(S$_2$PPr$^i_2$) | L*MoS(S$_2$PPh$_2$) |
|---|---|---|
| formula | $C_{24}H_{42}BMoN_6OPS_2$ | $C_{30}H_{38}BMoN_6PS_3$ |
| fw | 632.49 | 716.60 |
| space group | $P2_1/n$ | $P2_1$ |
| *a*, Å | 10.024(2) | 10.801(8) |
| *b*, Å | 20.999(9) | 13.100(5) |
| *c*, Å | 15.368(5) | 12.023(9) |
| $\beta$, deg | 100.57(2) | 99.56(10) |
| *V*, Å$^3$ | 3180(2) | 1678(2) |
| *Z* | 4 | 2 |
| $D_{calc}$, g·cm$^{-3}$ | 1.321 | 1.418 |
| no. of unique non-zero data used | 6148 | 4862 |
| no. of terms used for refinement | 5007 | 4600 |
| final no. of params refined | 386 | 402 |
| $R^a$ | 0.049 | 0.062 |
| $R_w$ | 0.050 | 0.080 |

[a] $R = \sum\Delta F/\sum|F_o|$, $R_w = [\sum w(\Delta F)^2/\sum w|F_o|^2]^{1/2}$.

(31) Macura, S.; Ernst, R. R. *Mol. Phys.* **1980**, *41*, 95.
(32) Bax, A.; Davis, D. G. *J. Magn. Reson.* **1985**, *65*, 355.
(33) Cromer, D. T.; Liberman, D. *J. Chem. Phys.* **1970**, *53*, 1891.

**Table 2.** Atomic Coordinates ($\times 10^4$) and Equivalent Isotropic Thermal Displacement Parameters ($Å^2 \times 10^3$) for L*MoO($S_2PPr^i_2$)

| atom | *x* | *y* | *z* | *U*(eq)[a] |
|---|---|---|---|---|
| Mo | −88(1) | 3164(1) | 7441(1) | 36(1) |
| S(1) | 2077(1) | 3071(1) | 8530(1) | 46(1) |
| S(2) | −182(1) | 4138(1) | 8364(1) | 49(1) |
| P | 1333(1) | 3742(1) | 9257(1) | 42(1) |
| O | −1038(3) | 2635(2) | 7865(2) | 53(1) |
| N(11) | 967(4) | 3815(2) | 6504(2) | 46(1) |
| N(12) | 653(3) | 3746(2) | 5596(2) | 41(1) |
| N(21) | −1822(3) | 3450(2) | 6415(2) | 42(1) |
| N(22) | −1751(3) | 3408(2) | 5535(2) | 43(1) |
| N(31) | 422(3) | 2467(2) | 6477(2) | 40(1) |
| N(32) | 97(3) | 2593(2) | 5582(2) | 42(1) |
| C(1) | 687(6) | 3417(3) | 10202(3) | 64(1) |
| C(2) | 1824(7) | 3133(3) | 10897(4) | 80(2) |
| C(3) | −496(7) | 2989(4) | 9967(4) | 99(2) |
| C(4) | 2635(5) | 4316(2) | 9757(3) | 55(1) |
| C(5) | 3386(7) | 4589(3) | 9072(4) | 81(2) |
| C(6) | 2056(7) | 4854(4) | 10247(5) | 99(2) |
| C(11) | 1886(6) | 4278(3) | 6644(3) | 61(1) |
| C(12) | 2178(6) | 4513(3) | 5851(3) | 67(2) |
| C(13) | 1373(4) | 4158(2) | 5193(3) | 49(1) |
| C(14) | 1266(6) | 4185(3) | 4203(3) | 61(1) |
| C(15) | 1590(9) | 4835(4) | 3896(5) | 110(3) |
| C(16) | 2119(9) | 3675(4) | 3889(5) | 111(3) |
| C(21) | −2965(5) | 3551(3) | 5054(3) | 56(1) |
| C(22) | −3851(5) | 3684(3) | 5612(3) | 60(1) |
| C(23) | −3102(4) | 3611(2) | 6473(3) | 50(1) |
| C(24) | −3594(5) | 3684(3) | 7335(3) | 65(1) |
| C(25) | −4696(8) | 3202(4) | 7407(5) | 97(2) |
| C(26) | −4087(7) | 4365(3) | 7435(4) | 87(2) |
| C(31) | 427(5) | 2090(2) | 5131(3) | 51(1) |
| C(32) | 957(6) | 1626(2) | 5714(3) | 59(1) |
| C(33) | 939(5) | 1880(2) | 6552(3) | 46(1) |
| C(34) | 1370(6) | 1551(2) | 7434(3) | 59(1) |
| C(35) | 363(8) | 1028(4) | 7555(4) | 98(2) |
| C(36) | 2795(7) | 1274(4) | 7512(5) | 100(2) |
| B | −421(5) | 3248(2) | 5229(3) | 42(1) |

[a] *U*(eq) is defined as one-third of the trace of the orthogonalized $\mathbf{U}_{ij}$ tensor.

The sites of the Mo, P, and S atoms for L*MoO($S_2PPr^i_2$) and the Mo, P, S, and most C atoms for L*MoS($S_2PPh_2$) were determined by direct [for L*MoO($S_2PPr^i_2$)] and Patterson [for L*MoS($S_2PPh_2$)] methods, followed by partial structure expansion using SHELXS86.[34] Subsequent difference syntheses using SHELX76[35] revealed the sites of all the remaining non-hydrogen atoms. The hydrogen atoms were included in the analyses at calculated positions and were assigned a variable overall isotropic thermal parameter. The structures were refined by the full-matrix least-squares method, with anisotropic parameters given to the non-hydrogen atoms. An anisotropic extinction parameter of the form $F_c = F[1 - (3.29 \times 10^{-7}|F^2|/(\sin\theta))]$ was applied to the calculated structure amplitudes of L*MoO($S_2PPr^i_2$).

Neutral atom scattering-factor curves for the non-hydrogen[36] and hydrogen[37] atoms were taken from the literature. Anomalous dispersion corrections were applied to the non-hydrogen atoms.[33] Final atomic positional coordinates for L*MoO($S_2PPr^i_2$) and L*MoS($S_2PPh_2$) are given in Tables 2 and 3, respectively. Selected bond distances and angles are presented in Table 4. Figures, drawn at the 25% probability level, were prepared from the output of ORTEP.[38]

(34) Sheldrick, G. M. SHELXS86, Program for Crystal Structure Solutions. *Acta Crystallogr.* **1990**, *A46*, 467.
(35) Sheldrick, G. M. *SHELX76 Program for Crystal Structure Determination*; Cambridge University: Cambridge, England, 1976.
(36) (a) Cromer, D. T.; Mann, J. B. *Acta Crystallogr.* **1968**, *A24*, 321. (b) Ibers, J. A.; Hamilton, W. C. *International Tables for X-Ray Crystallography*; Kynoch: Birmingham, England, 1974; Vol. 4, p 100. (c) Doyle, P. A.; Turner, P. S. *Acta Crystallogr.* **1968**, *A24*, 390.
(37) Stewart, R. F.; Davidson, E. R.; Simpson, W. T. *J. Chem. Phys.* **1965**, *42*, 3175.
(38) Johnson, C. K. ORTEPII. Report ORNL-5138; Oak Ridge National Laboratory: Oak Ridge, TN, 1976.

**Table 3.** Atomic Coordinates ($\times 10^4$) and Equivalent Isotropic Thermal Displacement Parameters ($Å^2 \times 10^3$) for L*MoS($S_2PPh_2$)

| atom | *x* | *y* | *z* | *U*(eq)[a] |
|---|---|---|---|---|
| Mo | 8591(1) | 10000 | 2035(1) | 35(1) |
| S | 8776(3) | 10805(3) | 3590(2) | 58(1) |
| S(1) | 6310(2) | 9575(2) | 1626(2) | 41(1) |
| S(2) | 8642(2) | 8194(2) | 2691(2) | 45(1) |
| P | 6773(2) | 8351(2) | 2637(2) | 38(1) |
| N(11) | 8656(6) | 9338(7) | 249(6) | 38(2) |
| N(12) | 9319(6) | 9790(6) | −482(6) | 38(2) |
| N(21) | 10608(6) | 10059(9) | 1952(6) | 39(2) |
| N(22) | 11010(7) | 10468(7) | 1029(7) | 44(2) |
| N(31) | 8354(6) | 11372(7) | 973(7) | 39(2) |
| N(32) | 9152(7) | 11568(7) | 224(7) | 43(2) |
| C(11) | 8080(9) | 8528(9) | −307(8) | 44(2) |
| C(12) | 8362(9) | 8471(9) | −1387(8) | 47(2) |
| C(13) | 9143(8) | 9287(9) | −1486(8) | 45(2) |
| C(14) | 9753(9) | 9607(10) | −2469(9) | 53(3) |
| C(15) | 9632(13) | 8756(16) | −3376(12) | 83(5) |
| C(16) | 9189(14) | 10613(14) | −3003(10) | 72(4) |
| C(21) | 12250(8) | 10515(9) | 1210(9) | 48(2) |
| C(22) | 12702(8) | 10124(13) | 2255(9) | 58(3) |
| C(23) | 11642(7) | 9829(9) | 2702(7) | 41(2) |
| C(24) | 11600(9) | 9371(11) | 3845(9) | 54(3) |
| C(25) | 12161(11) | 10092(16) | 4775(10) | 71(4) |
| C(26) | 12280(13) | 8332(14) | 3967(12) | 76(4) |
| C(31) | 8910(10) | 12512(9) | −238(9) | 48(2) |
| C(32) | 7954(10) | 12934(9) | 237(10) | 52(2) |
| C(33) | 7619(9) | 12211(9) | 983(9) | 45(2) |
| C(34) | 6611(9) | 12297(10) | 1721(10) | 51(3) |
| C(35) | 6987(11) | 13056(14) | 2655(10) | 70(4) |
| C(36) | 5335(10) | 12555(11) | 1031(11) | 62(3) |
| C(41) | 6366(8) | 8572(9) | 4029(8) | 45(2) |
| C(42) | 6351(11) | 7764(11) | 4749(10) | 58(3) |
| C(43) | 6057(12) | 7936(14) | 5841(10) | 69(4) |
| C(44) | 5828(11) | 8908(15) | 6198(10) | 71(4) |
| C(45) | 5845(10) | 9715(12) | 5464(10) | 65(4) |
| C(46) | 6106(9) | 9556(10) | 4385(9) | 52(3) |
| C(51) | 5929(8) | 7213(8) | 2130(9) | 43(2) |
| C(52) | 6508(10) | 6385(9) | 1730(10) | 53(2) |
| C(53) | 5813(12) | 5544(10) | 1291(12) | 65(3) |
| C(54) | 4512(12) | 5511(10) | 1290(10) | 60(3) |
| C(55) | 3955(10) | 6314(11) | 1680(10) | 60(3) |
| C(56) | 4612(9) | 7173(10) | 2121(10) | 53(3) |
| B | 10086(10) | 10762(10) | −44(9) | 40(2) |

[a] *U*(eq) is defined as one-third of the trace of the orthogonalized $\mathbf{U}_{ij}$ tensor.

## Results and Discussion

**Syntheses and Characterization of Oxo− and Thio−Mo(IV) Complexes.** Reaction of K{HB($Pr^ipz)_3$} with MoO($S_2PR_2$)$_2$ (R = $Pr^i$, Ph) in refluxing toluene produced the green, diamagnetic, oxo−Mo(IV) complexes, L*MoO($S_2PR_2$), which were isolated in ca. 60% yield following column chromatographic purification (Scheme 1). The syntheses follow the methodology developed for related $LMo^{IV}O$(dithoacid) complexes.[17,19,22] These complexes are air and water stable, readily soluble in chlorinated solvents and insoluble in alcohols, ethers, and hydrocarbons. Reaction of L*MoO($S_2PR_2$) with boron sulfide resulted in the production of the yellow-brown, diamagnetic, thio−Mo(IV) species, L*MoS($S_2PR_2$) (Scheme 1). The thio complexes were purified by flash chromatography followed by recrystallization; yields of ca. 50% were typical. Their synthesis finds precedent in the synthesis of $LMo^{IV}S(S_2CNR_2)$ complexes from their oxo analogues.[19] These complexes are slightly air-sensitive and were stored under an atmosphere of dinitrogen. They are soluble in chlorinated and aromatic hydrocarbons, slightly soluble in acetonitrile and insoluble in alcohol and ether solvents.

The alleviation of an unfavorable steric clash between the in-plane pyrazole and $R_{anti}$ dithiophosphinate substituent favors

**Table 4.** Interatomic Distances (Å) and Angles (deg) for L*MoO($S_2PPr^i_2$) and L*MoS($S_2PPh_2$)[a]

| atoms | L*MoO($S_2PPr^i_2$) | L*MoS($S_2PPh_2$) |
|---|---|---|
| Mo−E | 1.671(3) | 2.126(3) |
| Mo−S(1) | 2.494(1) | 2.494(2) |
| Mo−S(2) | 2.501(1) | 2.492(3) |
| Mo−N(11) | 2.372(4) | 2.328(8) |
| Mo−N(21) | 2.205(3) | 2.198(6) |
| Mo−N(31) | 2.207(4) | 2.195(8) |
| P−S(1) | 2.024(2) | 2.024(4) |
| P−S(2) | 2.029(2) | 2.019(3) |
| E−Mo−S(1) | 100.1(1) | 103.3(1) |
| E−Mo−S(2) | 103.8(1) | 101.5(1) |
| E−Mo−N(11) | 165.9(1) | 169.4(2) |
| E−Mo−N(21) | 91.7(2) | 94.2(2) |
| E−Mo−N(31) | 92.3(2) | 95.2(2) |
| S(1)−Mo−S(2) | 78.6(1) | 79.6(1) |
| S(1)−Mo−N(11) | 91.3(1) | 85.1(2) |
| S(1)−Mo−N(21) | 167.5(1) | 162.3(2) |
| S(1)−Mo−N(31) | 96.8(1) | 93.0(2) |
| S(2)−Mo−N(11) | 86.6(1) | 86.3(2) |
| S(2)−Mo−N(21) | 94.4(1) | 94.5(3) |
| S(2)−Mo−N(31) | 163.7(1) | 162.9(2) |
| N(11)−Mo−N(21) | 77.8(1) | 77.9(3) |
| N(11)−Mo−N(31) | 77.9(1) | 77.7(3) |
| N(21)−Mo−N(31) | 87.1(1) | 88.0(3) |
| Mo−S(1)−P | 87.3(1) | 85.5(1) |
| Mo−S(2)−P | 87.0(1) | 85.6(1) |
| S(1)−P−S(2) | 102.6(1) | 104.3(1) |

[a] The abbreviation E specifies the terminal oxo (O) and terminal thio (S) ligand in the complexes.

the formation of the L*MoO($S_2PR_2$) complexes (**A**) rather than their L′ analogues (**B**).[26] A number of $ML^*_2$ (M = $Fe^{II}$, $Co^{II}$, $Ni^{II}$) complexes have been reported by Trofimenko et al.[25] and

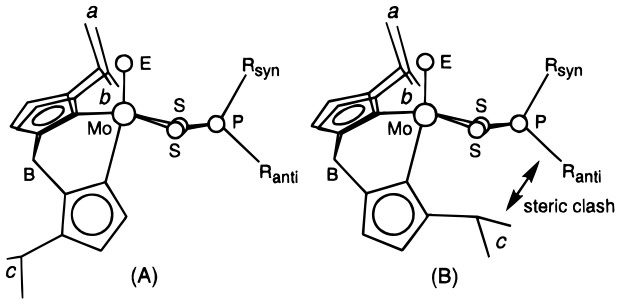


related ligands have been observed to undergo 1,2-boratropic rearrangements.[39−41] The observation of a novel "side-on" bonded pyrazole unit in $L_2U^{III}I$ provides an insight into how rearrangements of this type may be facilitated.[42] The relative rates of formation of L*MoO($S_2PR_2$) and LMoO($S_2PR_2$) complexes (minutes versus hours, respectively) may also reflect the capacity of the ligands to reduce steric interactions, especially in the transition states involved. The presence of the L* ligand was critical to the clean conversion of L*MoO($S_2PR_2$) to the thio complexes L*MoS($S_2PR_2$). All attempts to convert related LMoO($S_2PR_2$) and LMoO{$S_2P(OR)_2$} complexes to their thio analogues have proved unsuccessful;[21] while color changes consistent with the desired reactions with boron sulfide were consistently observed, a variety of workup procedures failed to secure the desired products. It is likely that the 3-isopropyl groups flanking the Mo═S group combine with the dithiophosphinate ligand to afford considerable protection to this moiety. To our knowledge only three other mononuclear thio−Mo(IV) complexes have been reported.[19,43,44]

The complexes were characterized by microanalytical, mass spectrometric, spectroscopic (Tables 5 and 6), and crystallographic techniques. The infrared spectra of L*MoO($S_2PR_2$) exhibit a strong single $\nu$(Mo═O) band at 955 $cm^{-1}$, a single $\nu$(BH) band at 2500 $cm^{-1}$, and other bands characteristic of the dithiophosphinate and pyrazolylborate ligands. The L*MoS($S_2PR_2$) complexes exhibit a single, medium intensity $\nu$(Mo═S) band at 515 $cm^{-1}$, a single $\nu$(BH) band at 2500 $cm^{-1}$, and other bands characteristic of the ligands. In the $\nu$(CN) region, these L* complexes exhibit two strong bands at 1510 and 1490 $cm^{-1}$, whereas L′$MoOCl_2$ and other L′ complexes exhibit a single, stronger and broader band at 1510 $cm^{-1}$.[16,45] This difference in the infrared spectra of L* and L′ complexes provides a quick and convenient indication of the ligand's regiochemistry.

The NMR spectra of the complexes are indicative of molecular $C_s$ symmetry, consistent with either structure **A** or **B** in solution. A priori, 1-D NMR cannot distinguish between these two structures but NOESY experiments confirmed structure **A**; full NMR assignments are given in Table 6 [Note: the crystallographic labeling schemes (vide infra) are employed to specify the protonic groups of L*, while the dithiophosphinate substituents are identified as $R_{syn}$ or $R_{anti}$ depending on their disposition relative to Mo═E (E = O, S)]. With the exception of L*MoO($S_2PPh_2$), the complexes exhibit three doublets of equal intensity in the $\delta$ 1.0−1.3 region; accidental equivalence accounts for the presence of two doublets of 2:1 intensity ratio in the spectrum of L*MoO($S_2PPh_2$). These doublet resonances are assigned to the methyl groups on the isopropylpyrazole fragments; the three symmetry related pairs, a and b (each diastereotopic) and c (enantiotopic) are indicated in structure **A**. A similar pattern would be predicted for structure **B**. The isopropyl methine groups of L* exhibit quite different chemical shifts in the two types of complex ($\Delta\delta$ 0.7 ppm when E = O, $\Delta\delta$ 1.5 ppm when E = S). In all cases, the less intense methine resonance, assigned to C(14)H, is considerably shielded relative to those of related L′ complexes (typically[16] $\delta$ >3.45). The doublet pyrazole ring-proton resonances ($\delta$ 5.5−8) exhibit a 2:1:2:1 intensity pattern and the $\delta$ 5.6 resonance is considerably shielded compared to resonances in related L′ complexes (typically[16] $\delta$ >6.06). The $\delta$ 6.95 resonances of L*MoS($S_2PR_2$) are also highly shielded within the series and in comparison to related L′ complexes. The shielded protons generally lie within the shielding zone associated with the terminal Mo═E group. For the L*MoE($S_2PPr^i_2$) complexes, two doublet of doublet resonances around $\delta$ 1.70 are assigned to the two pairs of enantiotopic methyl groups in the dithiophosphinate ligand; two doublet resonances are observed upon $^{31}P$ decoupling. The doublet of septet methine resonances associated with these ligands collapse to septet resonances upon $^{31}P$ decoupling. The phenyl resonances of the $S_2PPh_2^-$ ligand complexes ($\delta$ 7−8) are also simplified by $^{31}P$ decoupling (not analyzed in detail).

(39) Cano, M.; Heras, J. V.; Jones, C. J.; McCleverty, J. A.; Trofimenko, S. *Polyhedron* **1990**, *9*, 619.
(40) Cano, M.; Heras, J. V.; Trofimenko, S.; Monge, A.; Gutierrez, E.; Jones, C. J.; McCleverty, J. A. *J. Chem. Soc., Dalton Trans.* **1990**, 3577.
(41) Cano, M.; Heras, J. V.; Monge, A.; Pinilla, E.; Santamaria, E.; Hinton, H. A.; Jones, C. J.; McCleverty, J. A. *J. Chem. Soc., Dalton Trans.* **1995**, 2281.
(42) Sun, Y.; McDonald, R.; Takats, J.; Day, V. W.; Eberspacher, T. A. *Inorg. Chem.* **1994**, *33*, 4433.
(43) (a) Simhon, E. D.; Baenziger, N. C.; Kanatzidis, M.; Draganjac, M.; Coucouvanis, D. *J. Am. Chem. Soc.* **1981**, *103*, 1218. (b) Draganjac, M.; Simhon, E. D.; Chan, L. T.; Kanatzidis, M.; Baenziger, N. C.; Coucouvanis, D. *Inorg. Chem.* **1982**, *21*, 3321.
(44) Berreau, L. M.; Young, V. G., Jr.; Woo, L. K. *Inorg. Chem.* **1995**, *34*, 3485.
(45) (a) Xiao, Z.; Gable, R. W.; Wedd, A. G.; Young, C. G. *J. Chem. Soc., Chem. Commun.* **1994**, 1295. (b) Xiao, Z.; Gable, R. W.; Wedd, A. G.; Young, C. G. *J. Am. Chem. Soc.* **1996**, *118*, 2912.

**Table 5.** Spectroscopic and Electrochemical Data[a]

| compound | mass spectrum *m/z* (%) $[M]^+$ | infrared spectrum[b] KBr, $cm^{-1}$ $\nu$(CN) | infrared spectrum[b] KBr, $cm^{-1}$ $\nu$(MoE) | $^{31}P\{^1H\}$ NMR ($CDCl_3$) $\delta$ ($W_{1/2}$ Hz) | electronic spectrum $\lambda_{max}$ nm ($\epsilon$ $M^{-1}\cdot cm^{-1}$) ($CH_2Cl_2$) | cyclic voltammetry glassy carbon, $CH_3CN$ $E_{1/2}$, V ($\Delta E_{pp}$, mV; $I_{pa}/I_{pc}$) |
|---|---|---|---|---|---|---|
| L*MoO($S_2PPr^i_2$) | 634 (70) | 1510 s<br>1480 m | 955 s | 174 (50) | 670 (110), 405 (75) | +0.47 (87; 1.02) |
| L*MoO($S_2PPh_2$) | 702 (90) | 1510 s<br>1490 m | 955 s | 154 (35) | 660 (130), 430 (360 sh), 380 (930) | +0.52 (70; 1.02)<br>−1.80 (irrev) |
| L*MoS($S_2PPr^i_2$) | 650 (20) | 1510 s<br>1480 m | 515 s | 214 (65) | 395 (1500 sh), 325 (8800 sh) | +0.23 (71; 0.97)<br>−1.46 (irrev) |
| L*MoS($S_2PPh_2$) | 718 (60) | 1510 s<br>1490 m | 515 m | 190 (45) | 360 (2700 sh), 285 (10200) | +0.32 (62; 0.96)<br>−1.32 (irrev) |
| L*MoOS($S_2PPr^i_2$) | 666 (15)<br>634 (40)[c] | 1510 s<br>1480 m | 930 s | 110 (10) | 445 (1800), 335 (3850) | |
| L*MoOS($S_2PPh_2$) | 734 (20)<br>702 (45)[c] | 1510 s<br>1480 m | 930 s | 82 (10) | 450 (1700), 340 (3800) | |
| L′$MoOCl_2$ | | 1505 s | 975 s | | | |

[a] Complete listings of infrared data are given in the Experimental Section. [b] Intensities; s = strong, m = medium. [c] Due to $[M-S]^+$.

**Table 6.** $^1H$ NMR Data in $CDCl_3$ Solution[a]

| assignment | L*MoO($S_2PR_2$)[b] R = $Pr^i$ | L*MoO($S_2PR_2$)[b] R = Ph | L*MoS($S_2PR_2$)[b] R = $Pr^i$ | L*MoS($S_2PR_2$)[b] R = Ph | L*MoOS($S_2PR_2$)[c] R = $Pr^i$ | L*MoOS($S_2PR_2$)[c] R = Ph |
|---|---|---|---|---|---|---|
| $R_{syn}$ | 1.52 (dd, 7.0, 18)<br>2.89 (ds, 7.0, 6.8) | 7.93 (m, 2H)<br>7.48 (m, 3H) | 1.61 (dd, 7.0, 17)<br>3.91 (ds, 7.0, 14) | 8.12 (m, 2H)<br>7.54 (m, 3H) | 1.23 (dd, 7.0, 18)<br>1.23 (dd, 7.0, 18)<br>2.45 (ds, 7.0, 9) | 7.85 (m, 2H)<br>7.3−7.5 (m, 3H) |
| $R_{anti}$ | 1.48 (dd, 7.0, 18)<br>2.42 (ds, 7.0, 6.8) | 8.02 (m, 2H)<br>7.58 (m, 3H) | 1.59 (dd, 7.0, 17)<br>2.69 (ds, 7.0, 7.0) | 8.17 (m, 2H)<br>7.60 (m, 3H) | 1.45 (dd, 7.0, 18)<br>1.53 (dd, 7.0, 18)<br>3.22 (ds, 7.0, 7) | 7.92 (m, 2H)<br>7.3−7.5 (m, 3H) |
| C(11)H | 7.79 (d, 1.6) | 7.20 (d, 1.6) | 7.32 (d, 1.6) | 6.95 (d, 2.0) | 7.08 (d, 2.4) | 7.22 (d, 2.4) |
| C(21)H | 7.66 (d, 2.4) | 7.66 (d, 2.4) | 7.72 (d, 2.4) | 7.76 (d, 2.4) | 7.63 (d, 2.4) | 7.62 (d, 2.4) |
| C(31)H | | | | | 7.64 (d, 2.8) | 7.64 (d, 2.4) |
| C(12)H | 5.79 (d, 1.6) | 5.60 (d, 1.6) | 5.58 (d, 1.6) | 5.48 (d, 2.0) | 5.69 (d, 2.4) | 5.69 (d, 2.4) |
| C(22)H | 6.14 (d, 2.4) | 6.14 (d, 2.4) | 6.26 (d, 2.4) | 6.30 (d, 2.4) | 6.19 (d, 2.4) | 6.17 (d, 2.4) |
| C(32)H | | | | | 6.18 (d, 2.8) | 6.15 (d, 2.4) |
| C(14)H | 3.22 (sep, 6.8) | 3.18 (sep, 6.8) | 3.09 (sep, 7.0) | 3.15 (sep, 7.0) | 3.20 (sep, 6.8) | 3.19 (sep, 2.4) |
| C(24)H | 3.95 (sep, 6.8) | 3.95 (sep, 6.8) | 4.49 (sep, 6.8) | 4.54 (sep, 7.0) | 4.36 (sep, 6.8) | 4.31 (sep, 2.4) |
| C(34)H | | | | | 4.29 (sep, 6.8) | 4.08 (sep, 2.4) |
| $C(15)H_3$ | 1.17 (d, 6.8) | 1.11 (d, 6.8) | 1.07 (d, 7.0) | 1.07 (d, 7.0) | 1.14 (d, 6.8) | 1.14 (d, 6.8) |
| $C(16)H_3$ | | | | | 1.14 (d, 6.8) | 1.14 (d, 6.8) |
| $C(25)H_3$ | 1.23 (d, 6.8) | 1.23 (d, 6.8) | 1.20 (d, 7.0) | 1.23 (d, 7.0) | 1.39 (d, 6.8) | 1.39 (d, 6.8) |
| $C(35)H_3$ | | | | | 1.33 (d, 6.8) | 1.27 (d, 6.8) |
| $C(26)H_3$ | 1.22 (d, 6.8) | | 1.27 (d, 7.0) | 1.33 (d, 7.0) | 1.23 (d, 6.8) | 1.19 (d, 6.8) |
| $C(36)H_3$ | | | | | 1.19 (d, 6.8) | 1.08 (d, 6.8) |
| BH | 4.5 (br) | 4.5 (br) | 4.6 (br) | 4.6 (br) | 4.4 (br) | 4.5 (br) |

[a] With the exception of the $Ph_{anti}$ and $Ph_{syn}$ resonances, data are presented in the form: $\delta$ (multiplicity, $^3J_{HH}$ in Hz, $J_{PH}$ in Hz); the number of protons and carbon atoms to which they are attached are indicated in column 1 (see Figures 1, 2, and 4 for labeling schemes). Abbreviations: d = doublet, dd = doublet of doublet, ds = doublet of septets, m = multiplet, sep = septet, and br = broad. [b] For these complexes, available data do not permit unambiguous assignment of the $C(25)H_3/C(35)H_3$ and $C(26)H_3/C(36)H_3$ resonances. [c] For these complexes, available data do not permit the sets of resonances from the $Pr^i$pz groups containing N(21) and N(31) to be unambiguously distinguished (see text).

Two-dimensional NMR spectroscopy is able to distinguish between structures **A** and **B** and the assignments given in Table 6 are fully supported by NOESY and TOCSY experiments. NOESY spectra of the L*MoE($S_2PPr^i_2$) complexes reveal an NOE connectivity between the C(21)H/C(31)H resonance at ca. $\delta$ 7.7 and a broad resonance around $\delta$ 4.5, which we ascribe to the BH proton. This broad resonance also shows a weak NOE connectivity with the C(14)H resonance. These observations confirm that the unique pyrazole ring orients its isopropyl group toward the BH group rather than toward $Pr^i_{anti}$. The C(11)H resonance exhibits NOE connectivities with resonances at $\delta$ 2.45 and 1.48, which are accordingly assigned to the methine and enantiotopic methyl groups of $Pr^i_{anti}$, respectively. In the NOESY spectrum of L*MoO($S_2PPh_2$), NOE cross peaks between the broad BH resonance, the C(14)H resonance at $\delta$ 3.18, and the C(21)H/C(31)H resonance at $\delta$ 7.66, confirm the presence of L*. As well, NOE cross peaks between the phenyl ortho resonance at $\delta$ 8.02 and the C(11)H resonance at $\delta$ 7.20 identify this phenyl ortho resonance as that belonging to the $Ph_{anti}$ group; a further cross peak with the resonance at $\delta$ 7.58 identifies it as that belonging to the phenyl *m*- and *p*-protons of $Ph_{anti}$. The *o*-$Ph_{syn}$ resonances show a cross peak with the C(24)H/C(34)H resonance at $\delta$ 3.95. NOESY and TOCSY experiments confirmed the assignment of the resonance at $\delta$ 1.11 to the enantiotopic methyl groups c in structure **A**. The spectrum of L*MoS($S_2PPh_2$) was assigned by analogy to that of L*MoS($S_2PPr^i_2$). Available data do not permit the pairs of diastereotopic methyl groups a and b to be unambiguously assigned.

The electronic spectra of green L*MoO($S_2PR_2$) exhibit two d−d absorption bands at ca. 670 and 407−430 nm; the spectra are quite analogous to those of the corresponding LMoO($S_2PR_2$) complexes.[17] The tailing of intense UV LMCT bands into the visible accounts for the yellow-brown coloration of solutions of L*MoS($S_2PR_2$). Cyclic voltammograms in acetonitrile reveal a reversible oxidation at ca. +0.5 V for L*MoO($S_2PR_2$) and +0.23 to +0.32 V for L*MoS($S_2PR_2$). We show later that Mo(V) complexes, $[L^*Mo^VE(S_2PR_2)]^+$, are formed upon oxidation; the potentials are consistent with the reduced $\pi$-bonding capacity of the thio ligand compared to its oxo analogue.

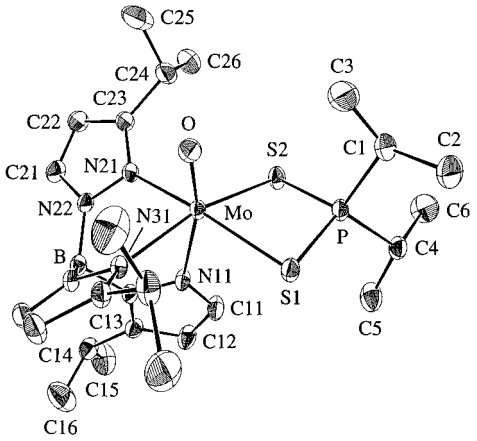


**Figure 1.** Molecular structure of L*MoO($S_2PPr^i_2$). The atom labeling scheme for the $Pr^i$pz group containing N(31) parallels that shown for the pseudo-mirror-related $Pr^i$pz group containing N(21).

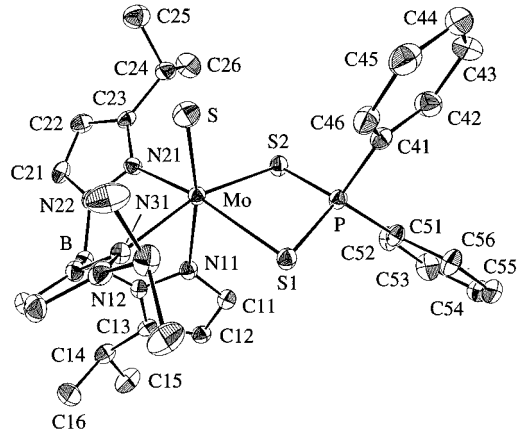


**Figure 2.** Molecular structure of L*MoS($S_2PPh_2$). The atom labeling scheme for the $Pr^i$pz group containing N(31) parallels that shown for the pseudo-mirror-related $Pr^i$pz group containing N(21).

Irreversible reductions were observed at ca. −1.8 and −1.4 V for L*MoO($S_2PR_2$) and L*MoS($S_2PR_2$), respectively. This behavior is very similar to that exhibited by LMoO($S_2PR_2$)[17] and related complexes.[19,22]

**Molecular Structures.** The molecular structures and atom labeling schemes for L*MoO($S_2PPr^i_2$) and L*MoS($S_2PPh_2$) are shown in Figures 1 and 2, respectively. The L*MoO($S_2PPr^i_2$) complex exhibits a distorted octahedral geometry and contains a terminal oxo ligand, a bidentate $S_2PPr^i_2{}^-$ ligand, and a facially tridentate L* ligand. The 5-$Pr^i$pz group of L* is coordinated *trans* to the Mo═O bond giving effective $C_s$ molecular symmetry. The Mo═O bond length of 1.671(3) Å is equal to the median value (1.67 Å) established for other oxo−Mo(IV) complexes.[19,46,47] The Mo═O bond exerts a strong *trans* influence on the Mo−N(11) bond, lengthening it by ca. 0.17 Å compared to the Mo−N bonds *cis* to the Mo═O unit. The Mo−S(1) and Mo−S(2) distances are slightly shorter than the median Mo−S distance in such complexes (2.535 Å).[47] The S(1), S(2), N(21), and N(31) atoms are approximately planar [maximum deviation 0.05 Å for N(21)] and the Mo atom is positioned 0.277 Å above this plane toward the oxo group. The phosphorus atom is 0.333 Å above the plane on the same side as the molybdenum atom, resulting in a hinging of the $MoS_2P$ fragment along the S··S vector. A dihedral angle of 23.5° is observed between the $MoS_2$ and $S_2P$ planes. The movement of the $Pr^i_{anti}$ group away from the region occupied by the 3-CH ring proton is likely to be responsible for the hinging effect. Steric interactions between the Mo═O and 3-$Pr^i$pz groups are reflected in a substantial increase in the N(21)−Mo−N(31) angle (87.1°) compared to the other N−Mo−N angles of ca. 77.9°.

The structure of L*MoS($S_2PPh_2$) is very similar to that described above for L*MoO($S_2PPr^i_2$). The Mo−S distance of 2.126(3) Å is typical of other thio−Mo(IV) complexes.[19,43,44,47] The thio ligand exerts a strong *trans* influence, lengthening the Mo−N(11) bond by ca. 0.13 Å compared to the other Mo−N bonds. The Mo−S(1) and Mo−S(2) distances are comparable to the values observed in L*MoO($S_2PPr^i_2$). The Mo and P atoms reside 0.341 and 0.312 Å, respectively, above (toward the thio ligand) the plane defined by S(1), S(2), N(21), and N(31) [maximum deviation of 0.011 Å for N(31)]. The $MoS_2P$ fragment is hinged along the S··S direction, the dihedral angle between the $MoS_2$ and $S_2P$ planes being 25.0°. This again reduces the steric interactions of the 3-CH and $Ph_{anti}$ groups. The larger than average N(21)−Mo−N(31) angle of 88.0(3)° accommodates the Mo═S group. In both complexes, the conformations of the $Pr^i$ groups of L* appear to be dictated by both intramolecular and intermolecular interactions.

**Synthesis and Characterization of Oxothiomolybdenum Complexes.** The L*MoO($S_2PR_2$) complexes were converted to orange, diamagnetic, oxo−thio−Mo(VI) complexes, L*MoOS-($S_2PR_2$-*S*), upon reaction with propylene sulfide in toluene at 55 °C (Scheme 1). The same compounds were generated when L*MoS($S_2PR_2$) were reacted with pyridine *N*-oxide in toluene at 55 °C (Scheme 1). The oxo−thio−Mo(VI) complexes are soluble in chlorinated and aromatic hydrocarbons, slightly soluble in acetonitrile and insoluble in alcohol and ether solvents. As well, NMR experiments revealed that samples of L*MoS-($S_2PR_2$) in $CDCl_3$ were converted to mixtures containing L*MoOS($S_2PR_2$) (ca. 60%) and L*MoO($S_2PR_2$) (ca. 40%) over a period of weeks in air. Reaction of L*MoS($S_2PPr^i_2$) with dry dioxygen in toluene at 50 °C produced a number of products including L*MoOS($S_2PPr^i_2$), L*MoO($S_2PPr^i_2$), and a blue complex with a striking TLC signature. The blue complex is tentatively identified as L*Mo($S_4$)($S_2PPr^i_2$), on the basis of its distinctive color and unusual NMR spectrum (Experimental Section). The extremely shielded resonances are assigned to an isopropyl group of L* which is located within the shielding zone associated with the $MoS_4$ ring.[10,48] Significant shielding is also experienced by the isopropyl groups of $S_2PPr^i_2{}^-$ which also occupy the shielding zone (on the opposite face of the $MoS_4$ ring from $Pr^i$pz). Since the complex has $C_1$ symmetry, a 5-$Pr^i$-pz group must flank the $MoS_4$ and $S_2PPr^i_2{}^-$ groups; the arrangement of ligands in the two enantiomers would be favored sterically. Reactions of L*MoS($S_2PR_2$) with $NBu_4NO_3$ or $H_2$-$NSO_3H$ form L*MoOS($S_2PR_2$) as well as significant amounts of L*MoO($S_2PR_2$). Reactions of L*MoS($S_2PR_2$) with propylene sulfide and L*MoO($S_2PR_2$) with oxygen atom donors were complicated either by the formation of numerous products or isomers; they were not further investigated.

Microanalytical and mass spectrometric data for L*MoOS-($S_2PR_2$) were consistent with their formulation as oxo−thio−Mo(VI) complexes. Two peak clusters assigned to the $[M]^+$ and $[M\text{-}S]^+$ ions were observed in the mass spectrum of each complex. UV−visible spectra, which exhibit absorptions at ca. 445 and 335 nm, are virtually identical to those of LMoOS($S_2$-

(46) Nugent, W. A.; Mayer, J. M. *Metal-Ligand Multiple Bonds*; Wiley: New York, 1988.

(47) Orpen, A. G.; Brammer, L.; Allen, F. H.; Kennard, O.; Watson, D. G.; Taylor, R. *J. Chem. Soc., Dalton Trans.* **1989**, S1.

(48) Reaction of L′$MoO_2Cl$ with $B_2S_3$ [cf. synthesis of LMo($S_4$)Cl[10]] produces a blue compound, formulated as L′Mo($S_4$)Cl, which exhibits NMR features related to some of those of L*Mo($S_4$)($S_2PPr^i_2$): $\delta$ −1.4 (sept, 1H), 0.2 (d, 6H), 1.27 (d, 6H), 1.73 (d, 6H), 4.44 (sept, 2H), 5.34 (d, 1H), 6.12 (d, 2H), 7.62 (d, 1H), 7.95 (d, 2H).

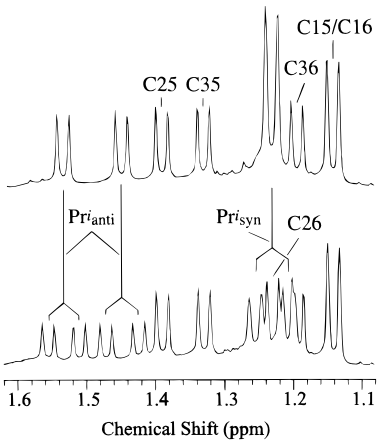


**Figure 3.** Methyl resonances in the NMR spectra of L*MoOS($S_2PPr^i_2$) in $CDCl_3$ at room temperature. Bottom: Fully coupled $^1H$ NMR spectrum. Top: $^{31}P$-decoupled $^1H$ NMR spectrum. The doublet of doublet resonances due to the four $S_2PPr^i_2{}^-$ methyl groups are simplified as indicated upon $^{31}P$-decoupling. Full assignments are given in Table 6.

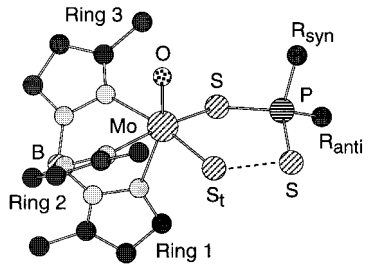


**Figure 4.** Structure of the L*MoOS($S_2PR_2$) complexes. For clarity, only the first carbon atom of each L* $Pr^i$ and dithiophosphinate R group is shown. The detailed numbering of the rings parallels that shown in Figures 1 and 2, e.g., ring 3 incorporates nitrogen and carbon atoms N(3*n*) and C(3*n*).

$PPr^i_2$) and related complexes.[21,23] The compounds exhibit a strong $\nu$(Mo═O) infrared absorption, a weak $\nu$(Mo═S) absorption and bands typical of the co-ligands. $^{31}P$ chemical shifts are typical of oxo−thio−Mo(VI) complexes of this type.[49] For both compounds, $^1H$ NMR spectra are consistent with the formation of a single major isomer with $C_1$ symmetry; data and assignments are given in Table 6. As shown in Figure 3, a complex set of resonances is observed in the methyl region of the $^1H$ NMR spectrum of L*MoOS($S_2PPr^i_2$). The spectrum in this region is dramatically simplified by $^{31}P$ decoupling, permitting the identification of the four $S_2PPr^i_2{}^-$ methyl resonances. The integrated intensities of the resonances confirm the presence of 10 methyl groups, although some coincidental overlap of chemical shifts is evident. Five isopropyl methine resonances are observed and two of these are simplified upon $^{31}P$ decoupling. Six doublet resonances are observed for the pyrazole ring protons of L*. The $^1H$ and $^1H\{^{31}P\}$ NMR spectra of L*MoOS($S_2PPh_2$) are similar to those of L*MoOS($S_2PPr^i_2$) with obvious differences due to the $S_2PR_2{}^-$ ligands. Both spectra are consistent with molecular $C_1$ symmetry for the L*MoOS($S_2PR_2$) complexes. $^{31}P$-Decoupled NOESY and TOCSY experiments (see Supporting Information) permitted the detailed assignments given in Table 6; the structure in Figure 4 was thereby established. A weak NOE cross peak between the C(21)H and C(31)H resonances at $\delta$ 7.64 and 7.63 and the broad BH resonance at $\delta$ 4.6, and the absence of a similar cross peak between the C(11)H and BH resonances, confirms the presence of the L* ligand. The C(*n*1)H ($\delta$ >7) and C(*n*2)H ($\delta$ 5.6−6.2) resonances are connected by both NOE and TOCSY cross peaks. An NOE cross peak between the C(12)H proton and the methyl resonance at $\delta$ 1.14 (intensity 6H) permits the assignment of the latter resonance to the C(15)$H_3$ and C(16)$H_3$ protons. These methyl protons also show a cross peak to the C(21)H and C(31)H resonances. A weak NOE cross peak, between the BH resonance and the septet resonance at $\delta$ 3.20, permits assignment of the latter to the C(14)H proton. The two methyl resonances at $\delta$ 1.43 and 1.53 are assigned to the $Pr^i_{anti}$ group by virtue of NOE cross peaks with the C(11)H resonance at $\delta$ 7.08; these also exhibit cross peaks to the $\delta$ 3.22 resonance assigned to the methine resonance of $Pr^i_{anti}$. A weak NOE connectivity is observed between the methine resonances of the $Pr^i_{syn}$ and $Pr^i_{anti}$ groups. $^1H\{^{31}P\}$ NOESY and TOCSY permit the assignment of *sets of resonances* to rings 2 and 3 (Figure 4) but not an unambiguous full assignment. Long-range NOEs between a particular 3-$Pr^i$ group and the $Pr^i_{syn}$ group, which would have permitted a definitive assignment, were not evident. The relatively shielded set of $Pr^i$pz resonances are (tenuously) assigned to the group bound *trans* to, and under the weak shielding influence of, the Mo═S group. An analogous assignment of the $^1H$ NMR spectrum of L*MoOS($S_2PPh_2$) is given in Table 6 (this assignment was not confirmed by 2D studies).

The mechanism of the reactions have not been probed directly but it is reasonable to suppose that atom transfer to L*MoO-($S_2PR_2$) and L*MoS($S_2PR_2$) is an associative bimolecular process, as observed for related processes.[17,21,22,50] Prior to or concomitant with the generation of the transition state complex, in which the atom-donor is bound to Mo, the bidentate dithiophosphinate ligand probably adopts a monodentate coordination mode and upon generation of the $[MoOS]^{2+}$ center becomes associated with the Mo═S unit through a weak S··S interaction.[23] OAT to either of the two potential oxo ligand binding sites *cis* to the thio group would produce enantiomers in which the 5-isopropylpyrazole group would flank the Mo═O group rather than being *trans* to the Mo═O group. At some stage along the reaction coordinate, boratropic shifts, or some other form of ligand rearrangement, must take place to form the observed, sterically favored enantiomeric products. SAT to one of the sites occupied by the bidentate $S_2PR_2{}^-$ ligand of L*MoO($S_2PR_2$) would produce directly the observed products.

**Generation of Mo(V) Complexes.** Reaction of L′$MoO_2$-Cl[16] with $PPh_3$ in dichloromethane resulted in the formation of the oxo−Mo(V) complex, L′$MoOCl_2$, in accord with previous results.[51] The reaction involves the initial formation of coordinatively unsaturated L′$Mo^{IV}OCl$ via OAT to $PPh_3$, followed by chlorine atom abstraction from $CH_2Cl_2$ and formation of L′$MoOCl_2$. The relatively small size of the oxo and chloro ligands permits the maintenance of the original conformation of the isopropylpyrazole groups. The presence of the L′ ligand is supported by infrared spectra and the inability of boron sulfide or $(Me_3Si)_2S$ to convert L′$MoOCl_2$ into the corresponding thio−Mo(V) complex. We ascribe the lack of reactivity to the steric protection afforded the Mo═O fragment by the three 3-isopropyl substituents. The EPR spectrum of L′$MoOCl_2$ is virtually identical to that reported by Cleland et al.[52] for $LMoOCl_2$.

(49) $^{31}P$ NMR data for $LMoOS(S_2PR_2)$: R = $Pr^i$, $\delta$ 108; R = Ph, $\delta$ 77 (from ref 21).

(50) Sulfur atom transfer from propylene sulfide to $LMoO(S_2PPr^i_2)$ in toluene obeys the second-order rate law $-d[LMoO(S_2PPr^i_2)]/dt = k[LMoO(S_2PPr^i_2)][C_3H_6S]$ with $k = 7.0(1) \times 10^{-6}$ $M^{-1}\cdot s^{-1}$ at 35 °C. The activation parameters for this reaction are $\Delta H^{\ddagger} = 61(1)$ kJ·mol$^{-1}$, $\Delta S^{\ddagger} = -142(2)$ J·K$^{-1}$·mol$^{-1}$ and $\Delta G^{\ddagger}$ 106(2) kJ·mol$^{-1}$ (at 35 °C) (from ref 21).

(51) Roberts, S. A.; Young, C. G.; Kipke, C. A.; Cleland, W. E., Jr.; Yamanouchi, K.; Carducci, M. D.; Enemark, J. H. *Inorg. Chem.* **1990**, *29*, 3650.

**Table 7.** EPR Parameters for the Mo(V) Complexes[a]

| complex | $g_{iso}$ | $A(^{95,97}Mo)$ | $a(^{31}P)$ | $a(^{1}H)$ |
|---|---|---|---|---|
| $[L^*MoO(S_2PPr^i_2)]^+$ | 1.963 | 42.5 | 36.9 | |
| $[L^*MoO(S_2PPh_2)]^+$ | 1.963 | 42.4 | 44.1 | |
| $[L^*MoS(S_2PPr^i_2)]^+$ | 1.961 | 44.3 | 36.5 | |
| $[L^*MoS(S_2PPh_2)]^+$ | 1.960 | 44.1 | 43.6 | |
| $L^*MoO(OH)(S_2PPr^i_2)$ | 1.950 | 45.0 | 12.2 | 12.2 |
| $L^*MoO(OH)(S_2PPh_2)$ | 1.949 | 44.7 | 12.5 | 12.5 |
| $L'MoOCl_2$ (THF) | 1.947 | 46.3 | | |

[a] Units of coupling constants = $10^{-4}$ $cm^{-1}$.

A number of EPR-active Mo(V) species were generated upon the oxidation of $L^*MoO(S_2PR_2)$ and $L^*MoS(S_2PR_2)$ (Scheme 1); EPR data and assignments are summarized in Table 7. The addition of substoichiometric quantities of $[FeCp_2]PF_6$ in dry $THF/CH_3CN$ (7:1) to THF solutions of $L^*MoO(S_2PR_2)$ (final Fe:Mo 1:19) produced orange-brown solutions which exhibited characteristic doublet EPR signals at $g$ ca. 1.963. The signals are assigned to the oxo−Mo(V) cations, $[L^*Mo^VO(S_2PR_2\text{-}S,S')]^+$. Oxidation of $L^*MoS(S_2PR_2)$ under the same conditions produced solutions containing the thio−Mo(V) cations $[L^*Mo^VS(S_2PR_2\text{-}S,S')]^+$, with $g$ ca. 1.961. Electrochemical oxidation of related $LMoS(S_2CNR_2)$ complexes is irreversible,[19] and the greater stability of $[L^*MoS(S_2PR_2)]^+$ may also be attributed to the increased steric protection afforded to the thio ligand by the L* ligand. The $g$ values for all four cationic species are very similar; however, a slightly lower $g$ value is characteristic of the thio complexes. The $LMo^VECl_2$ (E = O, S) complexes exhibit similar behavior, which is ascribed to the lowering of the HOMO−LUMO gap in the thio complexes relative to the oxo analogues.[18,53] The $g$ values for the oxo complexes are consistent with those of related cationic complexes containing L[17,21] and $H_2B(Me_2pz)_3^-$ ligands.[54] The complexes exhibit doublet Mo(V) EPR signals due to $^{31}P$ superhyperfine coupling. Coincidentally, the magnitude of the $^{31}P$ coupling is *nearly* equal to the $^{95,97}Mo$ hyperfine coupling, resulting in a spectrum in which all hyperfine lines exist as doublets except for the extreme lines which are singlets. Superhyperfine coupling to $^{31}P$ is dependent on its position relative to the magnetic orbital[17,55,56] and chelation of the dithio ligands permits significant coupling. The electron-withdrawing phenyl substituents of $[L^*MoO(S_2PPh_2)]^+$ and $[L^*MoS(S_2PPh_2)]^+$ enhance the $^{31}P$ coupling in these two complexes.

The addition of deoxygenated water to solutions of $[L^*MoO(S_2PR_2)]^+$ resulted in the generation of (hydroxo)oxo−Mo(V) species, $L^*Mo^VO(OH)(S_2PR_2\text{-}S)$, which exhibited characteristic triplet EPR signals;[17] these were stable for several hours under anaerobic conditions but were rapidly decomposed by dioxygen. Addition of deoxygenated $D_2O$ to solutions of $[L^*MoO(S_2PR_2)]^+$ resulted in the generation of species which exhibited doublet EPR signals assigned to the deuterated species $L^*MoO(OD)(S_2PR_2\text{-}S)$. Addition of $H_2O$ to solutions containing $[L^*MoS(S_2PR_2)]^+$ resulted in the production of several short-lived (minutes) EPR-active species. In the (hydroxo)oxo−Mo(V) species, the central resonance and the six hyperfine lines are split into a characteristic triplet signal indicating superhyperfine coupling to two spin-$^1/_2$ nuclei. In this case, a nonexchangable ligand $^{31}P$ and an exchangable hydroxo proton are the sources of coupling. Monodentate coordination in the (hydroxo)oxo complexes removes the phosphorus atom from the vacinity of the magnetic orbital and reduces the superhyperfine interaction; this is reflected in the lower $a(^{31}P)$ values compared to the cations above. The presence of $[Mo^VO(OH)]^{2+}$ species was confirmed by the generation of the deuterium analogue upon addition of $D_2O$ to solutions of $[L^*MoO(S_2PR_2)]^+$; these complexes exhibit the expected doublet signal produced by superhyperfine coupling to $^{31}P$ alone. Correlated electron−nucleophile transfer (CENT) reactions are involved in the formation of the $[Mo^VO(OH)]^{2+}$ species:[17,21]

$$L^*Mo^{IV}O(S_2PR_2) \rightarrow [L^*Mo^VO(S_2PR_2)]^+ + e^- \quad (4)$$

$$[L^*Mo^VO(S_2PR_2)]^+ + OH^- \rightarrow L^*Mo^VO(OH)(S_2PR_2) \quad (5)$$

Ferrocenium oxidation of oxo−Mo(IV) complexes in wet solvents also produces the $[Mo^VO(OH)]^{2+}$ species. The ability to independently observe the oxidation of Mo(IV), then the nucleophilic attack of $OH^-$ (or $H_2O$ initially) on Mo(V) implicates the CENT mechanism in this case as well. Related coupled electron−proton transfer (CEPT) reactions, involving prior coordination of $H_2O$ to the oxo−Mo(IV) species followed by oxidation and loss of a proton, produce (hydroxo)oxo−Mo(V) species in other systems:[16,57,58]

$$LMo^{IV}OX + H_2O \rightarrow LMo^{IV}OX(OH_2) \rightarrow [LMo^VOX(OH_2)]^+ + e^- \quad (6)$$

$$[LMo^VOX(OH_2)]^+ \rightarrow LMo^VOX(OH) + H^+ \quad (7)$$

The CEPT reactions are favored where X can function only as a monodentate ligand and where unsaturated $LMo^{IV}OX$ or weakly solvated $LMo^{IV}OX(solvent)$ complexes are generated, e.g., in OAT from $LMo^{VI}O_2(SPh)$ to $PPh_3$.[16,57,58] CEPT reactions are a specific example of a more general class of coupled electron−electrophile transfer (CEET) reactions;[57,58] i.e., the proton is the electrophile in CEPT reactions. The $[Mo^VO(OH)]^{2+}$ species produced by CENT are oxidized by dioxygen via a CEPT mechanism to EPR-silent species, presumably dioxo−Mo(VI) complexes.

The thio−Mo(V) cations, $[L^*MoS(S_2PR_2)]^+$, are potentially valuable precursors for oxothio−Mo(V) species and associated protonated species. Complexes of this type are implicated in the turnover of molybdenum enzymes such as xanthine oxidase and xanthine dehydrogenase. Unfortunately, extension of the CENT strategy to the generation of $[Mo^VS(OH)]^{2+}$ or $[Mo^VO(SH)]^{2+}$ species from $[L^*MoS(S_2PR_2)]^+$ was not realized. Addition of water to solutions of $[L^*MoS(S_2PR_2)]^+$ produced very short lived EPR-active species. The initial product, while likely to be $L^*Mo^VS(OH)(S_2PR_2)$, is rapidly transformed to thermodynamically favored $L^*Mo^VO(SH)(S_2PR_2)$. In the presence of water, these species are unstable with respect to dinuclear, EPR-silent $[L^*MoO]_2(\mu\text{-}O)(\mu\text{-}S_2)$.[59] Thus, unless actively stabilized, Mo═S groups, in the presence of water, undergo facile decomposition and/or dinucleation. Thus, ap-

(52) Cleland, W. E., Jr.; Barnhart, K. M.; Yamanouchi, K.; Collison, D.; Mabbs, F. E.; Ortega, R. B.; Enemark, J. H. *Inorg. Chem.* **1987**, *26*, 1017.
(53) An increase in the coordination-sphere sulfur content of oxo−Mo(V) complexes is invariably associated with an increase in the $g$ value of the complex. However, it is important to note that the "higher sulfur content, higher $g$ value" rule breaks down when oxo ligands are replaced by thio ligands, as in the present series and $LMoECl_2$.[18]
(54) Laughlin, L. J.; Gulbis, J. M.; Tiekink, E. R. T.; Young, C. G. *Aust. J. Chem.* **1994**, *47*, 471.
(55) Miller, G. A.; McClung, R. E. D. *Inorg. Chem.* **1973**, *12*, 2552.
(56) Chen, G. J.-J.; McDonald, J. W.; Newton, W. E. *Inorg. Chim. Acta* **1979**, *35*, 93.
(57) Xiao, Z.; Young, C. G.; Enemark, J. H.; Wedd, A. G. *J. Am. Chem. Soc.* **1992**, *114*, 9194.
(58) Xiao, Z.; Bruck, M. A.; Enemark, J. H.; Young, C. G.; Wedd, A. G. Submitted for publication.
(59) Xiao, Z.; Enemark, J. H.; Wedd, A. G.; Young, C. G. *Inorg. Chem.* **1994**, *33*, 3438.

plication of the CENT strategy in the synthesis of $[Mo^{V}O(SH)]^{2+}$ complexes from thio−Mo(IV) species is of limited value is this system.

**Summary.** Incorporation of the L* ligand into the oxo−Mo(IV) complexes L*MoO($S_2PR_2$) permits their conversion to stable, isolable thio−Mo(IV) complexes L*MoS($S_2PR_2$). Access to these thio−Mo(IV) species has allowed the first synthesis of stable, octahedral oxo−thio−Mo(VI) complexes via oxygen atom transfer to thio−Mo(IV) precursors. The synthesis of the same compounds via sulfur atom transfer to the oxo−Mo(IV) complexes confirms the formation of oxo−thio−Mo(VI) species in the OAT reactions. In the generation of all the complexes, the ability of the L* ligand to undergo boratropic or other rearrangements appears to be crucial to the stabilization of the ultimate products. As well, we have generated a number of oxo−Mo(V), thio−Mo(V) and (hydroxo)oxo−Mo(V) species via CENT reactions involving the oxo− and thio−Mo(IV) complexes. A (hydroxo)oxo−Mo(V) species is proposed as an intermediate in the regeneration of molybdoenzyme active sites.

**Acknowledgment.** We gratefully acknowledge the financial support of the Australian Research Council and the assistance of Simon Thomas, Zhiguang Xiao and Jason Hill.

**Supporting Information Available:** A composite figure of the NOESY and TOCSY spectra of L*MoOS($S_2PPr^i_2$) and full tables of crystallographic data, positional and displacement parameters, bond lengths, and bond angles for L*MoO($S_2PPr^i_2$) and L*MoS($S_2PPh_2$) (14 pages). Ordering information is given on any current masthead page.

IC960403T